DØnote 4742-CONF

Search for the Associated Production of Charginos and Neutralinos in the $\mu\tau + \ell$ Final State

The DØ Collaboration
URL http://www-d0.fnal.gov
(Dated: March 2, 2005)

Data collected from April 2002 through June 2004 by the DØ experiment in Run II of the upgraded Fermilab Tevatron Collider have been used to search for $\mu\tau_{had}+\ell$ final states accompanied by missing transverse energy. These topologies can contain contributions from the associated production of charginos and neutralinos. Data corresponding to an integrated luminosity of 326 pb^{-1} have been analyzed. Applying all selection criteria there is one event left in the data, consistent with the expectation from standard model backgrounds.

Preliminary Results for Spring 2005 Conferences

I. INTRODUCTION

Supersymmetry (SUSY [1]) postulates a symmetry between bosonic and fermionic degrees of freedom and predicts the existence of a supersymmetric partner for each Standard Model particle. In R-parity conserving models, SUSY particles are produced in pairs and the lightest supersymmetric particle (LSP) is stable. The following analysis is based on the supersymmetric extension of the Standard Model with minimal field content, the Minimal Supersymmetric Standard Model (MSSM) [1]. In this framework, the supersymmetric partners of charged and neutral Higgs and gauge bosons form two chargino ($\tilde{\chi}^{\pm}$) and four neutralino ($\tilde{\chi}^{0}$) mass eigenstates. At $p\bar{p}$ colliders, pairs of chargino and neutralino can be produced via an off-shell W boson. They decay into fermions and the LSP, leading to final states with jets, leptons and missing transverse energy ($\not\!\!E_T$) [2].

The following describes a search for final states containing a muon, a tau decaying hadronically, a third track, and missing transverse energy in data collected by the DØ experiment [3] at the Fermilab Tevatron collider. The pair production of charginos and neutralinos via an off-shell W boson in the s–channel or squark exchange in the t– and u–channels is expected to contribute to this topology.

The chargino decays into the lightest neutralino (LSP) and a virtual W boson if sleptons and sneutrinos are heavy. The W boson can decay according to its standard model branching ratio into a lepton and neutrino. If the sleptons are lighter than the chargino, a decay into a slepton and neutrino is favored. The slepton subsequently decays into the corresponding lepton and the lightest neutralino. The neutralino can decay into a Z–boson and the lightest neutralino. The decay of the Z–boson may lead to two more leptons in the final state. For small slepton masses, a decay of the neutralino into a slepton and lepton is also possible. Figure 1 shows the Feynman diagram for a possible decay with three leptons and missing transverse energy in the final state.

In SUSY-scenarios with high values of $\tan\beta$, the stau can be lighter than the selectron and smuon, so that the branching ratio for final states with three taus is much larger than for those with muons and electrons (Figure 2). The final state studied in the present analysis includes the decay into three taus, where one tau decays hadronically.

II. DATA AND MONTE CARLO SAMPLES

The data used in the present analysis were collected by the DØ experiment between April 2002 and June 2004. It corresponds to an integrated luminosity of (326±13) pb^{-1}. The luminosity is calculated by a normalization of the Monte Carlo to the Z-peak. A single muon trigger is used which requires a muon and a track with $p_T > 10$ GeV. Signal Monte Carlo has been generated for 36 different points in the mSUGRA parameter space. All points have been generated for $\tan\beta = 3$. The values for m_0 and $\mathrm{m}_{1/2}$ together with the corresponding cross sections and other parameters are listed in Table I. SUSY input parameters at the electroweak scale are obtained using Isajet version 7.58.

All Monte Carlo samples were generated with Pythia 6.202 [5], and processed through the full detector simulation and reconstruction chain. The background from multi–jet events is estimated from data by requiring an non-isolated muon. This multi–jet sample is normalized to the data sample.

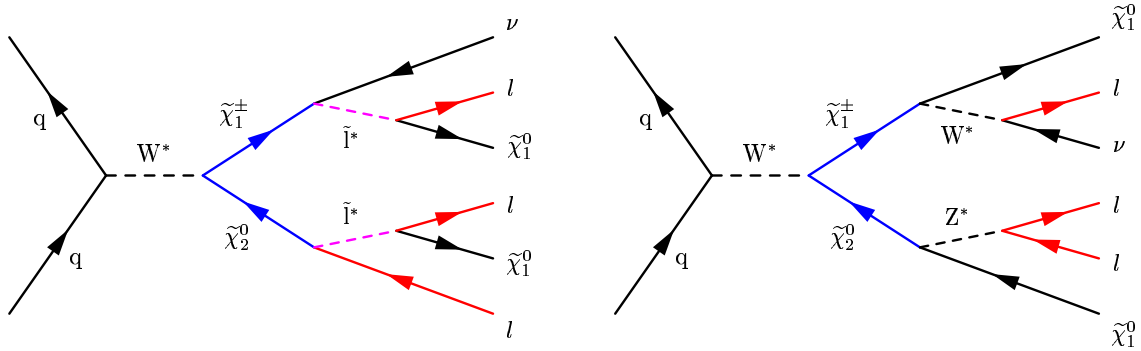

FIG. 1: Feynman diagram for the chargino/neutralino pair production in the s–channel and subsequent decay via sleptons (left) and gauge bosons (right).

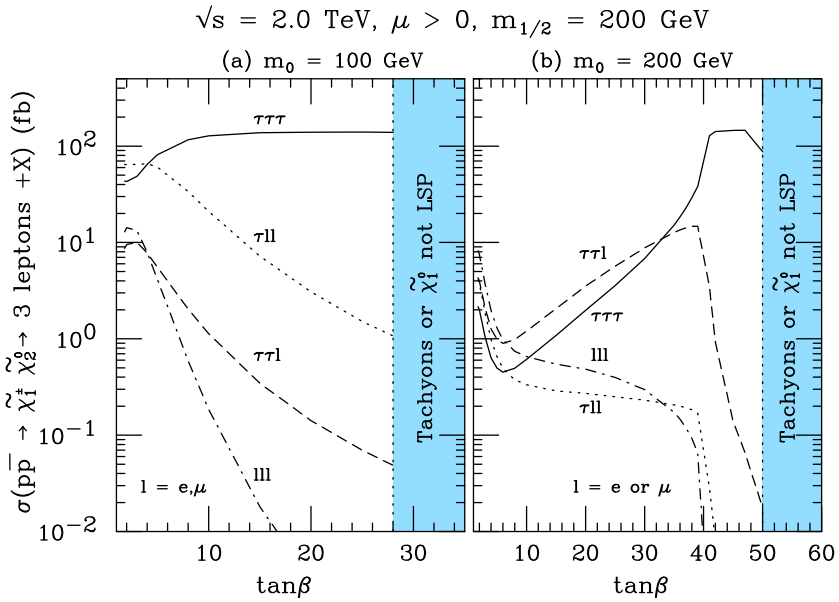

FIG. 2: Cross section for associated production of chargino and neutralino as function of $\tan\beta$. Figure taken from [4].

III. EVENT SELECTION

The event selection starts by requiring an isolated muon, which is matched to a track and has a transverse momentum larger then $p_T^\mu > 14$ GeV, and a τ decaying hadronically with a transverse momentum larger then $p_T^\tau > 7$ GeV. The tau is identified by using a neural net [6]. The tau is required to have a neural net output of $NN > 0.9$ (Figure 3), to originate from the same vertex as the muon and to pass a muon-veto, which consists of three cuts: $E/P > 0.5$, $CHF < 0.7$ and $\Delta R(\tau, \text{any } \mu \text{ in the event}) > 0.1$. CHF represents the fraction of energy deposition in the outer most part of the calorimeter [3].

As a cross check for the trilepton analysis in the $\mu+\tau+\ell$ final state and to test the tau identification, a comparison of the $Z/\gamma^* \to \tau\tau \to \mu\tau_{had}$ signal in data and Monte Carlo has been performed. The $Z/\gamma^* \to \tau\tau$ signal is elected by applying the following selection:

- $p_T^\tau > 25$ GeV
- Angle bewteen μ and $\not\!\!E_T$ $\Delta\phi(\mu, \not\!\!E_T) < 0.5$
- Missing transverse energy $\not\!\!E_T > 10$ GeV
- Transverse mass $m_T(\mu, \not\!\!E_T) < 8$ GeV
- opposite sign of μ and τ

The distribution of the angle is presented in Figure 3. The distribution of the invariant mass of the muon and tau is shown in Figure 4, including a distribution of the number of tracks of the tau. 178 events are observed in data, while in Monte Carlo 155 ± 12 events from $Z/\gamma^* \to \tau\tau$ plus 11 ± 1 events from background are selected. Events from "multi–jet" events dominate the background.

In the following selection of the SUSY signal, which is summarized in Table II, only 1–prong tau decays are used, since they have the highest purity.

The background from $Z/\gamma^* \to \mu\mu$ and $Z/\gamma^* \to \tau\tau$ is characterized by back-to-back topologies, so that a cut on $\Delta\phi(\mu, \tau) < 2.9$ rejects a large part of these events. $t\bar{t}$–events involving jets can be rejected using a cut on the scalar sum of the transverse momenta of all reconstructed jets $H_T < 80$ GeV. Since the signal contains a clear amount of $\not\!\!E_T$, a cut at $\not\!\!E_T > 20$ GeV is set, which rejects $Z/\gamma^* \to \tau\tau$, $Z/\gamma^* \to \mu\mu$ and multi–jet events. The $\not\!\!E_T$–distribution can be found in Figure 5. In events with jets the $\not\!\!E_T^{\text{scaled}}$ is defined as

$$\not\!\!E_T^{\text{scaled}} = \frac{\not\!\!E_T}{\sqrt{\sum_{\text{jets}} \left(\Delta E_{\text{jet}} \cdot \sin\theta_{\text{jet}} \cdot |\cos\Delta\phi\,(\text{jet}, \not\!\!E_T)\,|\right)^2}}, \tag{1}$$

TABLE I: Overview of the SUSY Monte Carlo with SUSY parameters and the production cross sections multiplied with the branching ratios. For all points: $A_0 = 0$ GeV and $\tan\beta = 3$.

Point	m_0 [GeV/c^2]	$m_{1/2}$ [GeV/c^2]	sign(μ)	$\sigma\times$BR [pb]	$m_{\tilde{\chi}_2^0}$ [GeV/c^2]	$m_{\tilde{\chi}_1^\pm}$ [GeV/c^2]	$m_{\tilde{\ell}_R}$ [GeV/c^2]	$m_{\tilde{\tau}_1}$ [GeV/c^2]	$m_{\tilde{\chi}_1^0}$ [GeV/c^2]	generated events
A1	56	165	+	1.032	102	98	92	90	55	20000
A2	64	165	+	0.771	102	98	97	95	55	21500
A3	72	165	+	0.388	102	98	102	101	55	17500
A4	80	165	+	0.349	102	98	108	106	55	18000
A5	88	165	+	0.290	102	98	114	112	55	18000
A6	200	126	–	0.057	102	103	208	207	52	22500
B1	60	170	+	0.858	106	101	96	94	58	18000
B2	68	170	+	0.663	106	101	101	99	58	20000
B3	76	170	+	0.316	106	101	106	105	58	25700
B4	84	170	+	0.283	106	101	112	110	58	21000
B5	92	170	+	0.236	106	101	118	117	58	21000
B6	200	132	–	0.048	106	107	209	207	54	22500
C1	64	175	+	0.727	110	106	99	98	60	21500
C2	72	175	+	0.555	110	106	105	103	60	22000
C3	80	175	+	0.261	110	106	110	109	60	23900
C4	88	175	+	0.232	110	106	116	115	60	23500
C5	96	175	+	0.191	110	106	122	121	60	24500
C6	200	138	–	0.040	110	111	210	208	57	19500
D1	68	180	+	0.604	114	110	103	101	62	25500
D2	76	180	+	0.467	114	110	109	107	62	21500
D3	84	180	+	0.213	114	110	114	113	62	25400
D4	92	180	+	0.188	114	110	120	119	62	21500
D5	100	180	+	0.141	114	110	126	125	62	23000
D6	200	142	–	0.036	114	114	210	208	58	21500
E1	72	185	+	0.512	118	114	107	105	65	31000
E2	80	185	+	0.402	118	114	112	111	65	21500
E3	88	185	+	0.176	118	114	118	117	65	22000
E4	96	185	+	0.153	118	114	124	123	65	22000
E5	104	185	+	0.126	118	114	130	129	65	37000
E6	200	148	–	0.031	118	119	211	209	61	20500
F1	90	205	+	0.256	135	132	124	123	74	14000
F2	98	205	+	0.180	135	132	130	129	74	19000
F3	106	205	+	0.074	135	132	136	135	74	18000
F4	114	205	+	0.068	135	132	142	141	74	15500
F5	122	205	+	0.057	135	132	148	147	74	28000
F6	200	166	–	0.018	135	132	212	211	69	18500

which gives an estimate of the impact of fluctuations of jet energy depositions on the $\not\!\!E_T$ [7]. $\not\!\!E_T^{\text{scaled}}$ is required to be greater than $8\ \sqrt{\text{GeV}}$. Events from multi–jet and Z/γ^* contributions can be rejected with a cut on the transverse mass $m_T^\mu > 20$ GeV and $m_T^\tau > 8$ GeV. The distribution of the transverse mass is presented in Figure 5.

The next step in the selection is the identification of a third track. A track is a clear signature of a charged lepton with the advantage that it is not affected by the reconstruction inefficiencies for an electron, a muon and a tau. The selection of the track is designed to be efficient for all three charged leptons. The track has to be well separated from μ and τ but coming from the same vertex. Its transverse momentum is required to be $p_T^{track} > 4$ GeV. In order to ensure its quality, only tracks are used with at least 17 hits in Silicon Microstrip Tracker (SMT) and Central Fiber Tracker (CFT) (if there is at least 1 CFT hit) or ≥ 14 CFT hits. Two isolation criteria are applied. The first one uses track information: $\sum p_T^{Track} < 1$ GeV in a hollow cone with $0.1 < R < 0.4$. The second one deals with the the calorimeter cells: $\sum E_T^{Cell} < 3$ GeV and $\sum E_T^{Cell} < 0.6 \times \sqrt{p_T^{track}}$ in a hollow cone with $0.2 < R < 0.4$. The distribution of p_T^{track} is shown in Figure 5.

After requiring the isolation track, the main backgrounds are $W^\pm \to \mu^\pm\nu$ and $Z/\gamma^* \to \mu\mu$, where in the second case the third track is coming from a non-reconstructed muon. These events passed the cuts dealing with $\not\!\!E_T$ because the muon was not reconstructed and consequentely $\not\!\!E_T$ is overestimated by the amount of the transverse momentum of the muon. A lot of the remaining $Z/\gamma^* \to \mu\mu$ events can be removed by cutting on the invariant mass of the muon and track (Figure 6). The cut is set at $M(\mu, track) < 60$ GeV. Another possibility to suppress $Z/\gamma^* \to \mu\mu$ events

is to cut on the transverse mass m_T^{track} of the third track and $\not\!\!E_T$. In cases where the third track originates from a non-reconstructed muon, $\not\!\!E_T$ points into the direction of the muon. This information can be used by requiring $m_T^{track} > 8$ GeV. If the track points into a region of the detector, where there are only one or two layers in the muon detector, the cut is tightened to $m_T^{track} > 15$ GeV. At this step of the selection, the major background is coming from $W^{\pm} \to \mu^{\pm}\nu$. Therefore a $p_T^{track} > 10$ GeV will be demanded, if the transverse mass $m_T(\mu, \not\!\!E_T)$ is located in the region of the W mass 50 GeV $< m_T^{\mu} <$ 95 GeV. A variable to reject background from multi–jets is the product of $\not\!\!E_T$ and p_T^{track}, since in multi–jet events both quantities tend to be small, while in the signal the product has large values (Figure 7 (left)). A cut is applied at $\not\!\!E_T \times p_T^{track} > 250$ GeV^2.

The cut $\not\!\!E_T \times p_T^{track} > 250$ GeV^2 is passed by a special set of $W^{\pm} \to \mu^{\pm}\nu$ events, which are characterized by large values of $\not\!\!E_T$. In order to get such large $\not\!\!E_T$ values, the W must be boosted. This is leading to a high-p_T muon coming from the W and a high-p_T jet in the opposite direction recoiling against the boson. The jet fakes the tau and in combination with the muon, a large invariant mass of muon and tau $M(\mu, \tau)$ is achieved. These events can be removed by requiring $M(\mu, \tau) < 120$ GeV. Another effective cut against multi–jet events is a cut on the product $p_T^{track} \times p_T^{\tau} > 150$ GeV^2 which is plotted in Figure 7 (right). Again for background the product is small, while it is large in the signal.

As during the last cuts of the cut flow, the background from WZ remains as the major background, two cuts are used to suppress it, exploiting the fact that the Z is decaying back-to-back into two leptons. If the Z decays into an electron pair, one electron will be identified as track, while the other will fake the tau. The invariant mass of μ and τ is used to remove this contamination: $M(\tau, track) < 75$ GeV. The influence of $Z \to \mu\mu$ and $Z \to \tau\tau$ can be suppressed by taking into account the angle between the two decay products $\Delta\phi(\mu, track) < 2.9$.

IV. RESULTS

The details of the contributions from different background sources are given in Table III, where it can be observed that the sum of the background events at every stage of the analysis is in agreement with the number of observed events. After all selection criteria are applied, one event is left in the data. This result is consistent with the sum of all the background events, which is $0.36 \pm 0.10(\text{stat.}) \pm 0.07(\text{syst.}) \pm 0.01(\text{lumi.})$ events. The display of this event is shown in Figure 8. Its properties are listed in Table IV. Various sources of systematic uncertainties have been studied to investigate their influence on signal efficiencies and background expectations, as summarized in Table V. The uncertainty is dominated by the limited statistics of the background samples.

V. CONCLUSION

A search for associated chargino and neutralino production has been performed, using the $\mu\tau_{had}\ell$ final state in DØ data recorded between April 2002 and June 2004. After all cuts there is one event left in data, which is consistent

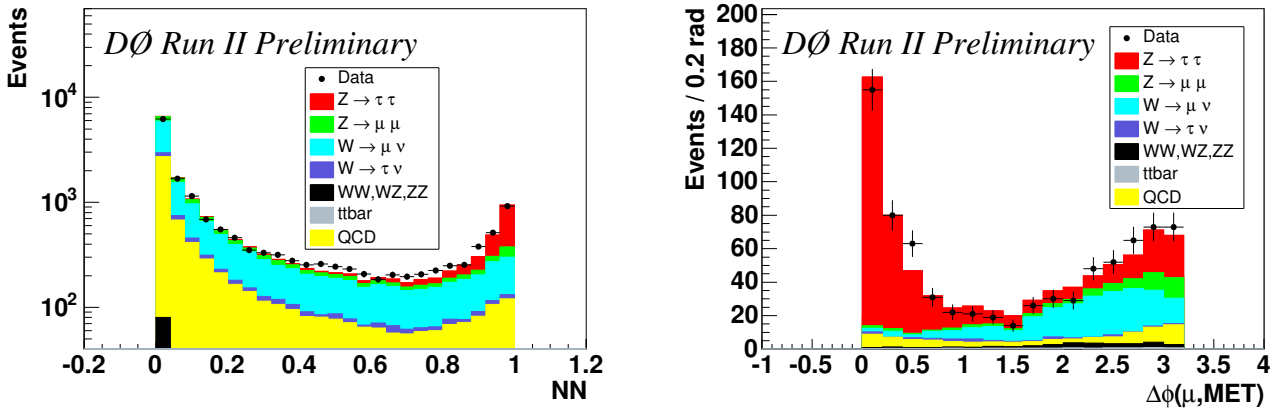

FIG. 3: Output of the neural net before cuts are applied. Distribution of the angle between μ and τ after $NN > 0.9$ for $p_T^{\tau} > 25$ GeV.

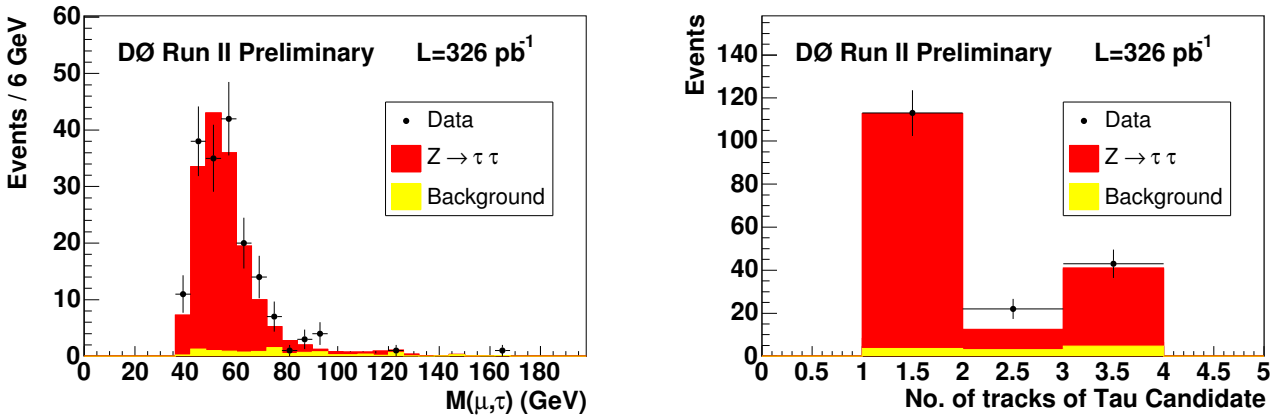

FIG. 4: Invariant mass $M(\mu,\tau)$ and number of tracks of the tau after cuts on $NN > 0.9$ and $\Delta\phi(\mu,\tau) < 0.5$ for events with $p_T^\tau > 25$ GeV.

TABLE II: Summary of the selection criteria.

	Selection criterion	Value
Cut 1	Preselection	Muon ID and Tau ID ($p_T^\mu > 14$ GeV, $p_T^\tau > 7$ GeV, $NN > 0.9$)
Cut 2	Z-Veto	$\Delta\phi(\mu,\tau) < 2.9$
Cut 3	$t\bar{t}$-Veto	$H_T < 80$ GeV
Cut 4	$\not\!\!E_T$ and m_T^μ	$\not\!\!E_T > 20$ GeV, $m_T^\mu > 20$ GeV, $\not\!\!E_T^{\rm Scaled} > 8\ \sqrt{\rm GeV}$
Cut 5	Third isolated track	$p_T^{track} > 3$ GeV
Cut 6	Transverse mass	$m_T^{track} > 8$ GeV, $(m_T^{track} > 15$ GeV$)^a$
Cut 7	Third isolated track	$p_T^{track} > 4$ GeV
Cut 8	Product of momenta	$\not\!\!E_T \times p_T^{track} > 250$ GeV^2
Cut 9	Z-Veto	$M(\mu, track) < 60$ GeV
Cut 10	W-Veto	$p_T^{track} > 9$ GeV, if 50 GeV $< m_T^\mu <$ 95 GeV, $M(\mu,\tau) < 120$ GeV
Cut 11	WZ-Veto	$M(\tau, track) < 75$ GeV, $\Delta\phi(\mu, track) < 2.9$
Cut 12	Transverse mass	$m_T^\tau > 8$ GeV
Cut 13	Product of momenta	$p_T^\tau \times p_T^{track} > 150$ GeV^2

[a]The cut will be tightend, if there are only one or two layers in the muon detector.

with expectations from standard model backgrounds. The analysis is not yet sensitive for a signal observation for any of the points under consideration. A combination with other channels ($ee\ell$, $\mu^+\mu^-\ell$, $e\tau\ell$ and same sign di–muon analyses) should increase the sensitivity.

Acknowledgments

We thank the staffs at Fermilab and collaborating institutions, and acknowledge support from the Department of Energy and National Science Foundation (USA), Commissariat à L'Energie Atomique and CNRS/Institut National de Physique Nucléaire et de Physique des Particules (France), Ministry for Science and Technology and Ministry for Atomic Energy (Russia), CAPES, CNPq and FAPERJ (Brazil), Departments of Atomic Energy and Science and Education (India), Colciencias (Colombia), CONACyT (Mexico), Ministry of Education and KOSEF (Korea), CONICET and UBACyT (Argentina), The Foundation for Fundamental Research on Matter (The Netherlands), PPARC (United Kingdom), Ministry of Education (Czech Republic), A.P. Sloan Foundation, Civilian Research and Development Foundation, Research Corporation, Texas Advanced Research Program, and the Alexander von Humboldt Foundation.

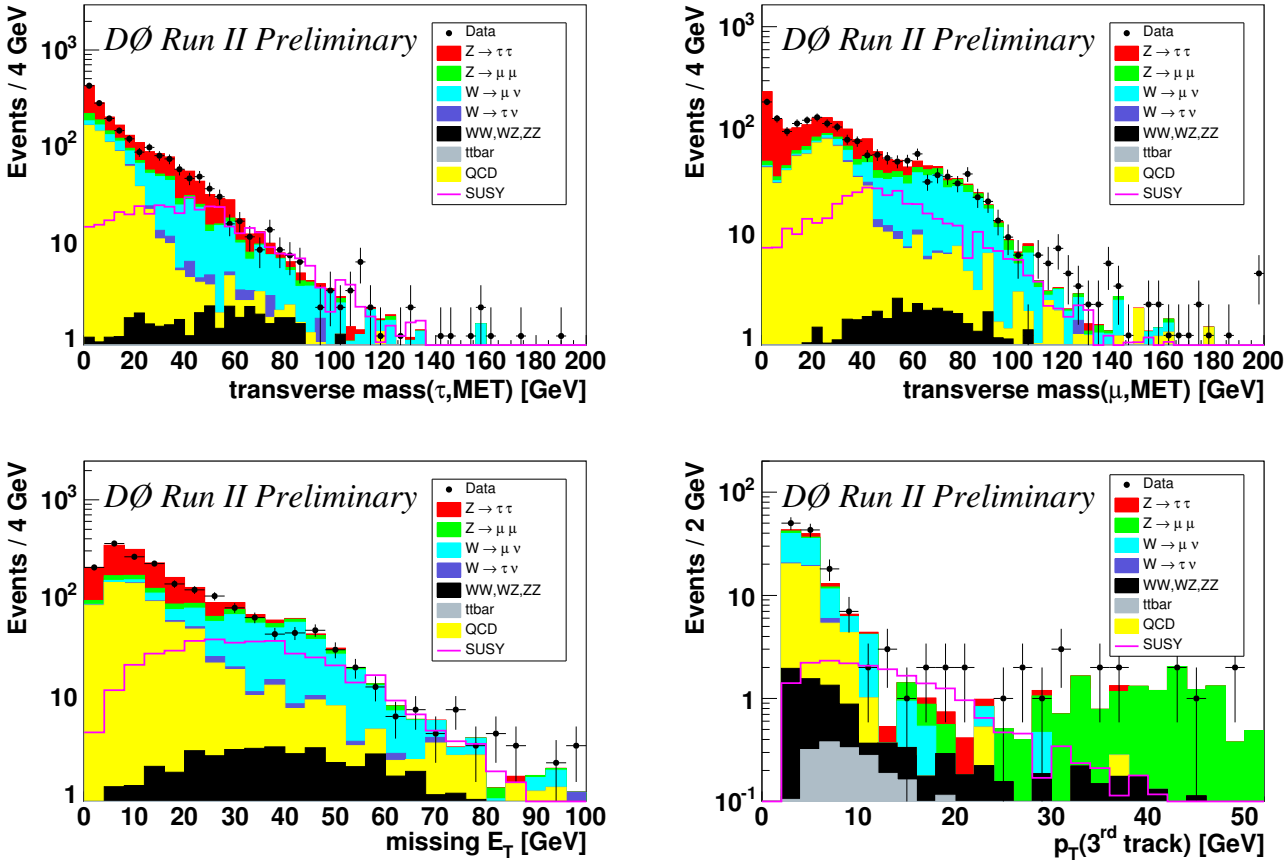

FIG. 5: m_T^τ, m_T^μ, and $\not\!\!E_T$ at the beginning of the selection (after Cut 1) and distribution of p_T^{track} at Cut 4. The line describes the signal of SUSY point D4 scaled by a factor of 100.

[1] H.P. Nilles, Phys. Rep. **110** (1984) 1;
H.E. Haber and G.L. Kane, Phys. Rep. **117** (1985) 75,

[2] W.Beenakker *et al.,* '*The production of Charginos/Neutralinos and Sleptons at Hadron Colliders* ",
hep-ph/9906298,

[3] DØ Collaboration, V. Abazov et al., "The Upgraded DØ Detector", in preparation for submission to Nucl. Instrum. Methods Phys. Res. A, and T. LeCompte and H.T. Diehl, Ann. Rev. Nucl. Part. Sci. 50, 71 (2000),

[4] Report of the SUGRA working group for Run II of the Tevatron
By SUGRA Working Group Collaboration (S. Abel et al.). FERMILAB-PUB-00-349, Mar 2000.

[5] T. Sjöstrand,
Comp. Phys. Comm **82**, 74, (1994).

[6] DØ Collaboration, First measurement of $\sigma(p\bar{p} \to Z)Br(Z \to \tau\tau)$ at $\sqrt{s} = 1.96$ TeV,
FERMILAB-PUB-04/381-E

[7] DØ Collaboration, "Search for the Associated Production of Chargino and Neutralino in Final States with Three Leptons',
DØnote 4738-CONF.

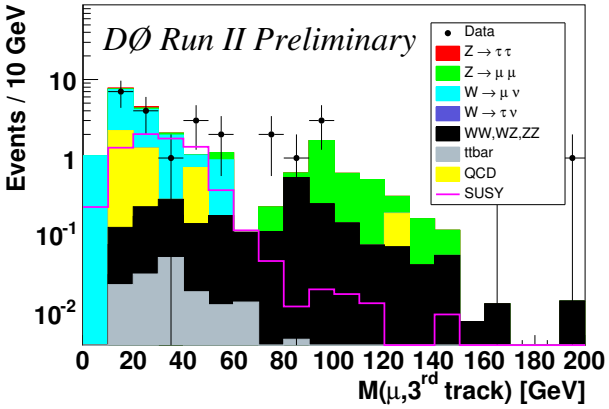

FIG. 6: Distribution of invariant mass of muon and track before the cut is applied. The line describes the signal of SUSY point D4 scaled by a factor of 5.

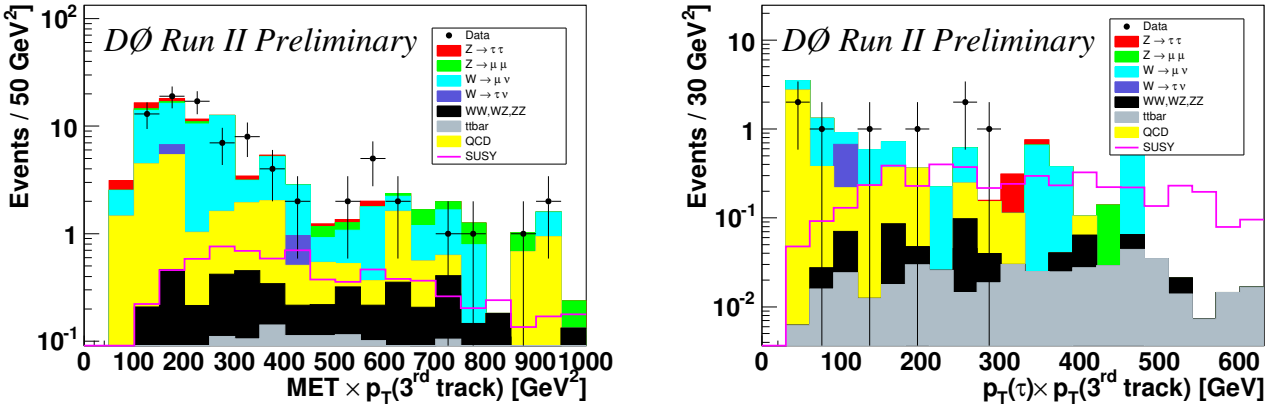

FIG. 7: Distribution of the products $\not\!\!E_T \times p_T^{track}$ (left) and $p_T^{\tau} \times p_T^{track}$ (right) before the corresponding cut is applied. Both distributions are plotted with loosened cuts in order to increase the statistics. The loosend cuts are chosen in a way they do not influence is considered distribution. The line describes the signal of SUSY point D4 scaled by a factor of 5.

TABLE III: Observed events and expected number of background events after successive steps of the selections for an integrated luminosity of $\int \mathcal{L}\mathrm{dt} = (326 \pm 13)$ pb^{-1}. The statistical error is listed for all backgrounds. The second row (*SUM*) contains the sum off all backgrounds, while in the last row the expectation of SUSY point D4 is documented.

	Cut 1	Cut 2	Cut 3	Cut 4	Cut 5	Cut 6
Data	1809	973	953	436	51	26
SUM	1878.38±20.49	1035.56±17.72	1012.91±17.57	444.66±12.07	41.33±3.47	22.48±2.98
QCD	626.69±13.7	434.14±12.76	422.24±12.6	79.42±5.76	5.05±1.21	3.87±1.08
$Z/\gamma^* \to \tau\tau$	697.34±8.93	146.26±4.14	143.41±4.09	10.61±1.13	0.78±0.34	0.33±0.23
$Z/\gamma^* \to \mu\mu$	115.46±3.68	63.83±2.81	63.59±2.8	27.77±1.64	14.92±1.31	3.52±0.6
W	398.09±11.73	357±11.18	354.32±11.14	301.64±10.37	17.12±2.95	12.25±2.69
WW	26.39±1.1	21.93±1	21.67±0.99	19.12±0.94	0.64±0.19	0.28±0.12
WZ	4.34±0.25	3.95±0.24	3.91±0.24	3.23±0.22	2.28±0.19	1.85±0.17
ZZ	1.32±0.09	1.06±0.08	0.95±0.08	0.5±0.06	0.33±0.05	0.21±0.04
$t\bar{t}$	8.75±0.13	7.39±0.12	2.82±0.07	2.37±0.06	0.21±0.02	0.17±0.02
D4	3.99±0.09	3.37±0.08	3.35±0.08	2.55±0.07	1.71±0.06	1.48±0.06

	Cut 7	Cut 8	Cut 9	Cut 10	Cut 11	Cut 12	Cut 13
Data	13	11	3	2	2	2	1
SUM	9.98±1.39	5.72±0.87	1.69±0.53	0.94±0.26	0.72±0.26	0.61±0.24	0.36±0.10
QCD	1.86±0.78	0.31±0.22	0.14±0.1	0.24±0.2	0.24±0.2	0.23±0.19	0.05±0.05
$Z/\gamma^* \to \tau\tau$	0.24±0.17	0.04±0.03	0.03±0.02	0.02±0.02	0.02±0.02	0.01±0.01	0.01±0.01
$Z/\gamma^* \to \mu\mu$	3.03±0.57	2.49±0.63	0.19±0.09	0.11±0.08	0.11±0.08	0.04±0.03	0.04±0.03
W	2.57±0.97	0.73±0.52	0.68±0.5	0.19±0.15	0.18±0.14	0.15±0.12	0.08±0.07
WW	0.11±0.08	0.05±0.05	0.05±0.05	< 0.05	< 0.05	< 0.05	< 0.05
WZ	1.85±0.17	1.79±0.17	0.47±0.08	0.3±0.06	0.13±0.04	0.13±0.04	0.13±0.04
ZZ	0.21±0.04	0.21±0.04	0.04±0.02	0.03±0.01	0.01±0.01	0.01±0.01	0.01±0.01
$t\bar{t}$	0.11±0.01	0.1±0.01	0.09±0.01	0.04±0.01	0.03±0.01	0.03±0.01	0.03±0.01
D4	1.4±0.06	1.21±0.05	1.16±0.05	1.01±0.05	0.89±0.05	0.87±0.05	0.79±0.04

TABLE IV: Properties of the event remaining after all cuts.

	p_T [GeV]	η	ϕ
Muon	46.73 GeV	-0.556	0.679
Tau (τ-type 2)	31.48	0.28	0.23
Track	5.13 GeV	1.61	5.89
$\not{E}_T$	74.46		3.57
Jet 1	40.05	0.80	3.67
Jet 2	15.22	2.60	0.69
$M(\mu,\tau)$	37.29 GeV	m_T^{μ}	117.04 GeV
$M(\mu, track)$	43.56 GeV	m_T^{τ}	96.37 GeV
$M(\tau, track)$	19.77 GeV	m_T^{track}	35.86 GeV

TABLE V: Influence of the various systematic variations on the background expectations and signal efficiency.

	Background	Signal
QCD normalization	15 %	–
Trigger efficiency	2 %	2 %
Muon reco correction	< 1 %	< 1 %
Muon track finding	< 1 %	< 1 %
Momentum calibration	1 %	1 %
Tau reco	6 %	6%
Signal cross sections	–	3.5 %
$W^{\pm} \to \mu^{\pm}\nu$-normalization	4%	–
Jet Energy Scale	12%	–
Sum	20 %	7 %
Luminosity	4%	4%

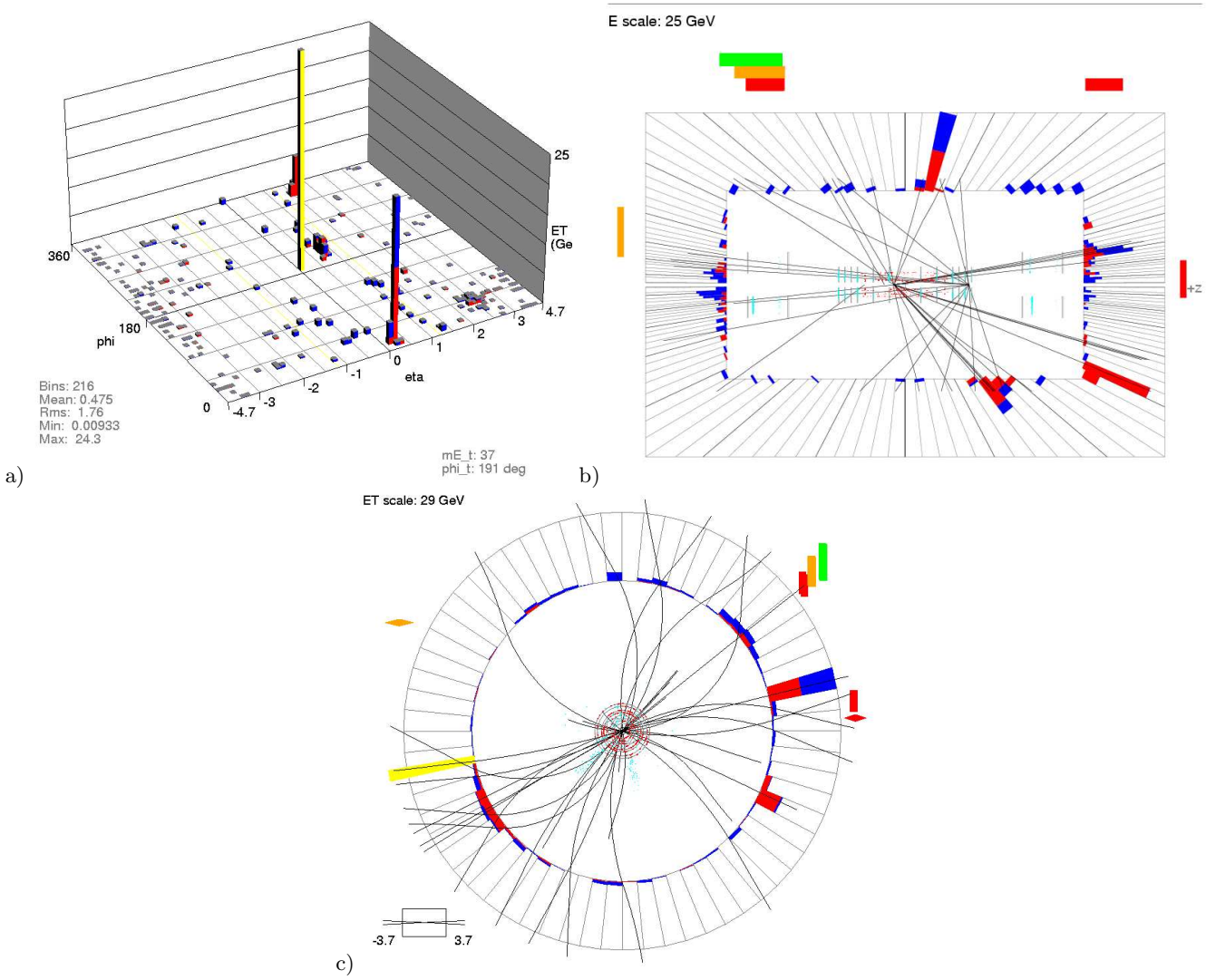

FIG. 8: Display of the selected event. a) Legoplot of the calorimeter inforamtion in the $\eta \times \phi$ plane. b) Side view (XY-plane) of the event with tracker information, calorimeter towers (red: electromagnetic energy, blue: hadronic energy, yellow: $\not\!\!E_T$) and signals of the muon chambers. c) Same as (b), but the RZ plane.